EXISTENCE AND STABILITY OF LIMIT CYCLES FOR PRESSURE OSCILLATIONS IN COMBUSTION CHAMBERS

E. Awad* and F. E. C. Culick**
California Institute of Technology
Pasadena, California

ABSTRACT

In this paper, we discuss two problems. First, using a second order expansion in the pressure amplitude, some analytical results on the existence, stability and amplitude of limit cycles for pressure oscillations in combustion chambers are presented. A stable limit cycle seems to be unique. The conditions for existence and stability are found to be dependent only on the linear parameters. The nonlinear parameter affects only the wave amplitude. The imaginary parts of the linear responses, to pressure oscillations, of the different processes in the chamber play an important role in the stability of the limit cycle. They also affect the direction of flow of energy among modes. In the absence of the imaginary parts, in order for an infinitesimal perturbation in the flow to reach a finite amplitude, the lowest mode must be unstable while the highest must be stable; thus energy flows from the lowest mode to the highest one. The same case exists when the imaginary parts are non-zero, but in addition, the contrary situation is possible. There are conditions under which an infinitesimal perturbation may reach a finite amplitude if the lowest mode is stable while the highest is unstable. Thus energy can flow "backward" from the highest mode to the lowest one. It is also shown that the imaginary parts *increase* the final wave amplitude.

Second, the triggering of pressure oscillations in solid propellant rockets is discussed. In order to explain the triggering of the oscillations to a non-trivial stable limit cycle, the treatment of two modes and the inclusion in the combustion response of *either* a *second* order nonlinear velocity coupling *or* a *third* order nonlinear pressure coupling seem to be sufficient.

INTRODUCTION

The limiting of the growth of pressure oscillations in combustion chambers has long been the object of investigation, but the best available data have been obtained with systems using solid propellants. Experimental results[1] with T-Burners show the general behavior most clearly : the pressure oscillation grows initially in time but, after few cycles, it levels off toward a limiting value known as a limit cycle. This is a pure nonlinear process for which the damping mechanism is amplitude dependent.

One classical example of the existence of limit cycles is the Van der Pol's oscillator[2], where the damping is amplitude dependent. Following this analogy, Culick[3] introduced the first theoretical interpretation of the limiting amplitude, of pressure oscillations in combustion chambers, by introducing a model of one nonlinear oscillator for which the nonlinear terms represent the wall losses and particle attenuation. But a detailed examination of the structure of the waveform of limit cycles confirmed that the process is more complicated. The waveform shows a distortion of the fundamental acoustic mode and involves generation of higher harmonics by different nonlinear processes, mainly the nonlinear gasdynamics of the flow. This is essentially the mechanism responsible for the formation of shock waves in fluid flow.

To explain the effect of the nonlinear gasdynamics on the formation of limit cycle, Culick[4] presented, for the first time, an approximate analysis for the contribution of this kind of nonlinearity. By expanding the pressure field in the normal acoustic modes of the chamber, he showed that the nonlinear behavior could be represented by a system of nonlinear oscillators. Using reference [4] as a basis, Jensen and Beckstead[5] examined the influence of the energy transfer among modes on the formation of limit cycles . They found that indeed the gasdynamics nonlinearity played a major role in establishing the limit cycle. As a means of checking the approximate analysis, Culick and Levine[6] integrated numerically the conservation equations in rocket chambers, using the method of characteristics. They found that for small pressure disturbances the approximate analysis yielded satisfactory results.

The major advantages of using the approximate analysis are first, the very low cost of computing the limit cycle, especially when it comes to three dimensional problems; and second, a solution, when possible, of the approximate analysis will yield a direct insight into the quantitive and qualitative influences of the different processes in the chamber. The major disadvantage is that, by definition, the method is approximate and therefore cannot represent accurately the different combustion processes. On the other

---

* Graduate Student

** Professor of Engineering, Associate Fellow, AIAA.

hand, the numerical analysis, while yielding in general, a more accurate representation costs much more and cannot explain easily either quantitatively or qualitatively, the role of each process in the chamber in establishing the limit cycle. From the point of view of physical understanding of the nonlinear instabilities in combustion chambers, an analytical solution will yield a deeper insight than the numerical solution.

Interest in dealing with the limiting amplitude in combustion chambers lies not only in interpreting some experimental data but in understanding the general behavior of pressure oscillations in combustion chambers. In fact, the results which will be elaborated in this paper are of general application and can be applied easily to any sort of combustion chambers (ramjet engines, solid and liquid propellant rocket, furnaces, etc.) . Here, we will apply the results to solid propellant rocket motors because of the availability of data.

None of the references cited above provides the answers to the following questions: when does a limit cycle exist? what are the effects of the linear parameters on the stability, existence, and amplitude of the limit cycles? and what is the effect of the nonlinear parameter?

The aim of this paper is to answer these questions by giving, while limiting the discussion to a finite number of modes, explicit analytical results.

In Section 1, we use a second order acoustic model to find the amplitude and the conditions for existence and stability of the limit cycle. Broadly, the analysis breaks into two parts. First, for a chosen type of limit cycle (there are two), the conditions for existence and the amplitudes are found. Then a perturbation procedure is used to examine the stability of the limit cycle.

In Section 1.1, we treat the case when the fundamental frequency of the limit cycle is equal to the fundamental frequency of the chamber. Section 1.1.1 deals with two modes only. The objectives are to calculate the amplitude and to determine the conditions for existence and stability of the limit cycle. The purpose is to explain the influence of the linear and nonlinear parameters on the formation of limit cycle. In order to examine the numerical results of Levine and Baum[7] who showed, numerically, the independence of the limit cycle on the initial conditions, we will show also analytically in this part how the initial conditions can change the stability of the limit cycle. The influence of the imaginary part of the linear responses on the final amplitude is demonstrated. The objective is to see how these imaginary parts alter the amplitude and the stability conditions of the limit cycle. The reason for studying this effect is the suspicion that the phase relationships between the pressure oscillations and the different processes in the chamber play a major role in the stability of the limit cycle. In section 1.1.2, we deal with three modes. The objectives here are to confirm the basic conclusions found in the treatment of two modes and to show how the analysis can be extended to any number of modes.

In Section 1.2, we treat the case when the fundamental frequency of the limit cycle is slightly different from the fundamental acoustic frequency of the chamber. The objective is to extend the results to a wider range of linear coefficients, thus making the application of the results to practical problems more accurate. Two modes are fully treated. In order to confirm the results, the case of three modes is treated only numerically.

Section 1.3 is a comparison between the analytical results on one hand and the numerical and experimental results, reported by other investigators, on the other hand. The main purpose of this part is to show how the analytical results can be applied to real problems, in order to understand the physical mechanisms behind the limiting amplitude phenomenon. Because of the availabilty of data on solid propellant rocket motors, these results will be applied solely to this kind of systems. But the validity and the scope of application are much wider and the results can be applied to any sort of chamber.

In Section 2, an analytical formulation, using a third order expansion in the pressure amplitude and treating two modes, for the triggering of pressure oscillations in solid propellant rockets is presented. In this section, we will show the major mechanisms responsible for triggering and how they effect this phenomenon. The reason for studying this problem is the realization that triggering, or nonlinear instability, is a general phenomenon and is not related to a particular chamber geometry or to a specific propellant. This is, to our knowledge, the first global analytical representation of triggering.

1. ANALYSIS

In reference [4], the pressure oscillation, written in the form

$$p' = \sum_{i=1}^{\infty} \eta_i \cos \omega_i x$$

is governed by the following system of nonlinear oscillators, one oscillator for each mode:

$$\ddot{\eta}_i + \omega_i^2 \eta_i = f_i(\eta_j, \dot{\eta}_j) \qquad (I)$$

i=1,2, ... , j=1,2, ..., and f_i is a second order nonlinear polynomial. By applying the method of averaging[4], the following system of ordinary differential equations is obtained

$$\frac{dA_n}{dt} = \alpha_n A_n + \vartheta_n B_n + n\frac{\beta}{2}\sum_{i=1}^{\infty}$$

$$\left[A_i(A_{n-i} - A_{i-n} - A_{n+i}) - B_i(B_{n-i} + B_{i-n} + B_{n+i})\right] \qquad (1)$$

$$\frac{dB_n}{dt} = \alpha_n B_n - \vartheta_n A_n + n\frac{\beta}{2}\sum_{i=1}^{\infty}$$

$$\left[A_i(B_{n-i} + A_{i-n} - B_{n+i}) + B_i(A_{n-i} - A_{i-n} + A_{n+i})\right] \qquad (2)$$

where $n = 1, 2, \ldots, \beta = \frac{\gamma+1}{8\gamma}\omega_1$ and $\eta_i(t) = A_i(t)\sin\omega_i t + B_i(t)\cos\omega_i t$

In what follows, we will treat two cases. First, the case when the coefficients A_i and B_i reach constant values for large time; and second, the case where A_i and B_i reach harmonic oscillations for large time. These cases yield periodic solutions of the form $\eta_i(t) = A_i(t)\sin\omega_i t + B_i(t)\cos\omega_i t$, and, therefore, they correspond to limit solutions. In Appendix A, we show that, under certain conditions, these two cases are the only possible ones. The first case corresponds to the case when the fundamental frequency of the limit cycle is equal to the fundamental frequency of the chamber and it will be referred to as " Zero shift of frequency case ". The second case corresponds to a slight difference of the fundamental frequency of the limit cycle from the fundamental acoustic frequency of the chamber and it will be referred to as " Non-zero shift of frequency case".

1.1. Case of zero shift of frequency

In this part, we will consider the case when the coefficients A_i and B_i in $\eta_i(t) = A_i(t)\sin\omega_i t + B_i(t)\cos\omega_i t$ will reach constant values for $t \to \infty$. The system to be solved is the following

$$\alpha_n A_n + \vartheta_n B_n + n\frac{\beta}{2}\sum_{i=1}^{\infty}$$

$$\left[A_i(A_{n-i} - A_{i-n} - A_{n+i}) - B_i(B_{n-i} + B_{i-n} + B_{n+i})\right] = 0.$$

$$\alpha_n B_n - \vartheta_n A_n + n\frac{\beta}{2}\sum_{i=1}^{\infty}$$

$$\left[A_i(B_{n-i} + A_{i-n} + B_{n+i}) + B_i(A_{n-i} - A_{i-n} + A_{n+i})\right] = 0.$$

1.1.1. Two modes . First, the case of two nonlinear oscillators is fully treated. The system (1)-(2) becomes

$$\alpha_1 A_1 + \vartheta_1 B_1 - \beta\,(A_1A_2 + B_1B_2) = 0. \qquad (3)$$

$$-\vartheta_1 A_1 + \alpha_1 B_1 + \beta\,(B_1A_2 - A_1B_2) = 0. \qquad (4)$$

$$\alpha_2 A_2 + \vartheta_2 B_2 + \beta\,(A_1^2 - B_1^2) = 0. \qquad (5)$$

$$-\vartheta_2 A_2 + \alpha_2 B_2 + 2\beta B_1A_1 = 0. \qquad (6)$$

Write A_i and B_i as follows

$A_i = r_i\cos\nu_i, \qquad B_i = r_i\sin\nu_i, \qquad i=1,2.$

Equations (3)-(6) reduce to

$$\frac{\alpha_1}{\cos\psi_1} r_1\cos(\nu_1-\psi_1) - \beta r_1 r_2\cos(\nu_1-\nu_2) = 0 \qquad (7)$$

$$\frac{\alpha_1}{\cos\psi_1} r_1\sin(\nu_1-\psi_1) + \beta r_1 r_2\sin(\nu_1-\nu_2) = 0 \qquad (8)$$

$$\frac{\alpha_2}{\cos\psi_2} r_2\cos(\nu_2-\psi_2) + \beta r_1^2\cos 2\nu_1 = 0 \qquad (9)$$

$$\frac{\alpha_2}{\cos\psi_2} r_2\sin(\nu_2-\psi_2) + \beta r_1^2\sin 2\nu_1 = 0 \qquad (10)$$

where

$$\psi_i = \text{Arctan}\,\frac{\vartheta_i}{\alpha_i}, \qquad i=1,2$$

This system yields

$$\tan(\nu_1-\psi_1) = -\tan(\nu_1-\nu_2), \quad \tan(\nu_2-\psi_2) = \tan 2\nu_1$$

which has the solutions

$$\nu_2 = 2\nu_1 - \psi_1 + m\pi \qquad (11)$$

and

$$\nu_2 = 2\nu_1 + \psi_2 + n\pi \qquad (12)$$

Therefore, in order for the solution to be unique, we should have

$$\psi_1 + \psi_2 = (m - n)\pi$$

But, by definition of the Arctan, $-\frac{\pi}{2} < \psi_1 < \frac{\pi}{2}$, giving

$$\psi_1 = -\psi_2$$

This is equivalent to

$$\frac{\vartheta_1}{\alpha_1} = -\frac{\vartheta_2}{\alpha_2} \qquad (13)$$

Taking into account (12)-(13), we find from equations (7)-(10)

$$r_2 = \frac{\alpha_1}{\beta\cos\psi_1}, \qquad r_1^2 = -\frac{\alpha_1\alpha_2}{\beta^2\cos\psi_1\cos\psi_2}$$

Since $-\frac{\pi}{2} < \psi_1 < \frac{\pi}{2}$, we should have

$$\alpha_1\alpha_2 < 0. \qquad (14)$$

The condition (14) assures the existence of the limit cycle and it shows clearly the necessity of having both a source and a sink of energy. The amplitude of the limit cycle can be expressed via the values of A_i and B_i

$$A_i = r_i\cos\nu_i, \qquad B_i = r_i\sin\nu_i, \qquad i=1,2.$$

Since the system (I) of nonlinear oscillators is autonomous, i.e., if $\eta(t)$ is a solution then $\eta(t - t_1)$ is also a solution for any t_1. And, since we are dealing with the asymtotic solution (limit cycle), assumed to be periodic, one phase in the expansion of the limit cycle in its Fourier components is arbitrary. This is equivalent to say that one of the ν_i is arbitrary, say $\nu_1 = 0$. That gives

$$A_{10} = \frac{1}{\beta\cos\psi_1}(-\alpha_1\alpha_2)^{\frac{1}{2}}$$

$$= \frac{1}{\beta}\left(-\alpha_1\alpha_2\left(1 + \frac{\vartheta_1^2}{\alpha_1^2}\right)\right)^{\frac{1}{2}}$$

$$B_{10} = 0.$$

$$A_{20} = \frac{\alpha_1}{\beta}$$

$$B_{20} = \frac{\vartheta_1}{\beta}$$

Once the equilibrium points A_{i0} and B_{i0}, $i = 1,2$, are found, their stability can be carried out by linearizing the system (3)-(7) near these points. The eigenvalues of the linear system should all have negative real parts. Linearization of (3)-(7) produces the following equations:

$$\frac{dA_1}{dt} = (\alpha_1 - \beta A_{20})A_1 + (\vartheta_1 - \beta B_{20})B_1$$

$$-(\beta A_{10})A_2 - (\beta B_{10})B_2$$

$$\frac{dB_1}{dt} = (-\vartheta_1 - \beta B_{20})A_1 + (\alpha_1 + \beta A_{20})B_1$$

$$+(\beta B_{10})A_2 - (\beta A_{10})B_2$$

$$\frac{dA_2}{dt} = (2\beta A_{10})A_1 - (2\beta B_{10})B_1$$

$$+\alpha_2 A_2 + \vartheta_2 B_2$$

$$\frac{dB_2}{dt} = (2\beta B_{10})A_1 + (2\beta A_{10})B_1$$

$$-\vartheta_2 A_2 + \alpha_2 B_2$$

By writing $A_1 = U_1 e^{\lambda t}$, etc., where U_1, etc., are constant, and replacing these expressions in the above linear system we get a linear system of equations for U_1, etc., of the form

$$M\vec{X} = 0$$

where M is the matrix of the linear system and $\vec{X}$ represent U_1, etc. This system has non-zero solutions only when its determinant vanishes. This gives a polynomial equation in λ, the characteristic polynomial. For the system in question, the characteristic polynomial is

$$P(\lambda) = \lambda^4 - 2\lambda^3(\alpha_1 + \alpha_2) + \lambda^2(\alpha_2^2 + \vartheta_2^2 + 4\vartheta_1\vartheta_2)$$

$$+\lambda\, 2\alpha_1\alpha_2(2\alpha_1 + \alpha_2)\left(1 + \frac{\vartheta_2^2}{\alpha_1^2}\right) \qquad (15)$$

The conditions under which the limit cycle is stable are reduced to those under which all the roots of this polynomial have negative real parts. Many textbooks treat this problem (see [8] for example). These conditions are commonly known as Routh-Hurwitz or Liénard criteria. For a polynomial of the form

$$P(\lambda) = \lambda^4 + a_3\lambda^3 + a_2\lambda^2 + a_1\lambda$$

these criteria are

$$a_1 > 0,\ a_3 > 0,\ a_2a_3 - a_1 > 0.$$

a) $\vartheta_1 = \vartheta_2 = 0$

The case when $\vartheta_1 = \vartheta_2 = 0$ is first carried out to completion. $P(\lambda)$ is, thus, reduced to

$$P(\lambda) = \lambda^4 - 2\lambda^3(\alpha_1 + \alpha_2) + \lambda^2(\alpha_2^2)$$

$$+ \lambda(2\alpha_1\alpha_2^2 + 4\alpha_1^2\alpha_2).$$

The stability conditions are then given, by applying Liénard criteria,

$$\alpha_1+\alpha_2 > 0$$

$$4\alpha_1^2\alpha_2 + 2\alpha_1\alpha_2^2 > 0$$

$$4\alpha_1\alpha_1^2 + 4\alpha_1^2\alpha_2 - 2\alpha_2^3 > 0.$$

These conditions reduce to

$$2\alpha_1 + \alpha_2 < 0 \qquad (16)$$

$$\alpha_1 + \alpha_2 > 0 \qquad (17)$$

$$\alpha_1 > 0. \qquad (18)$$

To these one must add the existence condition (14). The results are shown in Figure 1. As we see from the graph, in order to get a stable limit cycle, *the first mode should be unstable. The second mode should be stable and should decay at least twice as fast as the growth of the first mode.*

Without the nonlinear coupling, the first mode is unstable, thus supplying energy (source of energy) to the wave; the second mode is stable, thus extracting energy (sink of energy) from the wave. The nonlinearity coupling channels the energy from the first mode to the second mode. We say that the energy flows from the first to the second mode. When the limit cycle is reached, the sink and source of energy cancels each other.

To demonstrate the independence of the limit cycle on general initial conditions, Figures 2a and 2b show, by integrating the system of ordinary differential equations, the behavior in time of the amplitude of different harmonics for different initial conditions. Figures 3a and 3b show the influence of the linear damping coefficient α_2 on how fast the limit cycle is reached and on the limiting amplitude. It is concluded that the higher the damping is, the faster the limit cycle is reached and the higher the amplitude of the first mode is. Figure 4b shows the behavior in time of the pressure amplitude when the conditions (16)-(18) are not satisfied; it is clearly seen that, while the existence condition (14) is satisfied, the limit cycle is unstable, i.e., it cannot exist numerically. That was predicted by the analytical results (16)-(18).

In all these examples, the numerical results agree completely with the predicted analytical ones in the sense that the numerical solution of the system of ordinary differential equations yields the same behavior predicted by the analysis regarding: existence, stability and amplitude of limit cycles.

In the following part, it will be shown that the initial conditions, under very special circumstances, can change the stability criteria (16)-(18). Let us assume that the initial conditions are of the following form

$$B_1(0) = B_2(0) = 0.$$

and that ϑ_1, ϑ_2 both vanish. The direct conclusion is that the two modes are in phase. This will be shown to be the reason for reducing the stability criteria. Equations (3)-(7) , in this case, become

$$\alpha_1A_1 - \beta A_1A_2 = 0. \qquad (19)$$

$$\alpha_2A_2 + \beta A_1^2 = 0. \qquad (20)$$

B_1 and B_2 vanish for all times. System (19)-(20) has the following solution

$$A_{10} = \frac{\sqrt{(-\alpha_1\alpha_2)}}{\beta}, \quad A_{20} = \frac{\alpha_1}{\beta}$$

By linearizing the system (19)-(20) near the above solution, it is easily shown that the stability criterion is simply

$$\alpha_1 > 0, \quad \alpha_2 < 0. \qquad (21)$$

The criterion (21) is much less restrictive than the criteria (16)-(18). However, the initial conditions here are very restrictrive. The criteria (16)-(18) are the general

ones under general initial conditions. Figure 4b, in comparison with Figure 4a, illustrates clearly the influence of the initial conditions on the stability criteria (16)-(18). The only differences between these two Figures are the initial conditions; in Figure 4b, where the initial conditions are not in phase, the limit cycle is unstable as predicted by the stability criteria (16)-(18); in Figure 4a, where the initial conditions are in phase, the limit cycle is stable as predicted by the criterion (21).

b) $\vartheta_1, \vartheta_2 \neq 0$

Now, we treat the case for ϑ_1 and ϑ_2 different from zero, while always satisfying the condition (13) for zero shift of frequency. The point is to show that the stability criteria (16)-(18) are still valid but are not necessary. It will be shown that the imaginary parts affect greatly the stability and amplitude of the limit cycle. Ultimately, the direction of flow of energy among modes will depend on these imaginary parts.

In order for the characteristic polynomial (15) to have all roots with negative real parts, the following conditions, using Liénard criteria as before, should simultanuously be satisfied

$$\alpha_1 + \alpha_2 < 0.$$

$$2\alpha_1 + \alpha_2 < 0.$$

$$2\alpha_2\vartheta_2^2\left(-\frac{\alpha_1^2}{\vartheta_1^2} - 3 + 2\frac{\alpha_1}{\alpha_2^2}(2\alpha_1 + \alpha_2)\right) > 0.$$

The first two conditions amount to the same conditions (16)-(17) found for the case $\vartheta_1 = \vartheta_2 = 0$. But the third condition implies two possibilities. First $\alpha_2 < 0$; this case yields the same result (18) found for $\vartheta_1 = \vartheta_2 = 0$. Second, $\alpha_2 > 0$; this case yields the following stability condition

$$\alpha_2 < 2\frac{\alpha_1(2\alpha_1 + \alpha_2)}{\alpha_2(3 + \frac{\alpha_1^2}{\vartheta_1^2})} \qquad (22)$$

This condition shows clearly that it is possible to get a stable limit cycle when the first mode is stable and the second mode is unstable. In conclusion, the conditions (16)-(18) are *sufficient* here but *not necessary*.

To illustrate the results, Figure 5 shows an example of numerical integration of the system of ordinary differential equations when the first mode is stable and the second mode is unstable and when the criterion (22) is satisfied but the criteria (16)-(18) are not. The limit cycle in this case is stable, in contradiction to the stabiltity criteria (16)-(18) but consistent with the criterion (22).

In the case when the first mode is stable (sink of energy) and the second mode is unstable (source of energy), the nonlinear coupling channels the energy from the second to the first mode. The direct conclusion here is that the energy can flow "backward" from the higher to the lower modes. Whether this occurs depends on the values of $(\vartheta_1,\vartheta_2)$ which correspond to the imaginary parts of the combustion responses.

This is, up to our knowledge, the first time such effect is shown. The imaginary parts do indeed play a major role in the process of limiting the pressure oscillations in combustion chambers. Relying only on the real parts of the responses of the different processes in the chamber yields insufficient, sometimes misleading, information about the limiting amplitude process.

1.1.2. Three modes .

Now, the system of 3 nonlinear oscillators will be treated. A general approach for solving a system of many nonlinear oscillators can be constructed. The purpose of this section is to show that a stable limit cycle is unique and that the analysis can be carried out to any number of oscillators. Write

$$Z_j = A_j + i\,B_j \quad j=1,2,3.$$

where $i = \sqrt{-1}$. Thus, for a system of 3 nonlinear oscillators, system (1) and (2) gives, when the limit cycle is reached,

$$\frac{\alpha_1}{\cos\psi_1} e^{i\psi_1} Z_1^* - \beta\,(Z_1 Z_2^* + Z_2 Z_3^*) = 0$$

$$\frac{\alpha_2}{\cos\psi_2} e^{i\psi_2} Z_2^* + \beta\,(Z_1^{*2} - 2 Z_1 Z_3^*) = 0$$

$$\frac{\alpha_3}{\cos\psi_3} e^{-i\psi_3} Z_3 + 3\,\beta\, Z_1 Z_2 = 0\,.$$

where * stands for complex conjugate. Elimination of Z_3 yields

$$\frac{\alpha_2}{\cos\psi_2} e^{i\psi_2} Z_2^* + \beta\,(Z_1^{*2} + 6\,\beta\frac{Z_1 Z_1^* Z_2^* \cos\psi_3\, e^{i\psi_3}}{\alpha_3}) = 0.$$

Elimination of Z_2 gives, for $y = Z_1 Z_1^*$,

$$c_0\, y^2 + c_1\, y + c2 = 0 \qquad (23)$$

where

$$c_0 = 3\beta^4 \cos\psi_3 \, e^{-i\psi_3} + 36\beta^4 \frac{\alpha_1}{\alpha_2} \frac{\cos^2\psi_3}{\cos\psi_1} e^{i\psi_1}$$

$$+ 18\beta^4 \cos\psi_3 \, e^{i\psi_3}$$

$$c_1 = 12\beta^2 \alpha_1 \frac{\alpha_2}{\alpha_3} \frac{\cos\psi_3}{\cos\psi_1 \cos\psi_2} \cos(\psi_2 + \psi_3) \, e^{i\psi_1}$$

$$+ 3\beta^2 \frac{\alpha_2}{\cos\psi_3} e^{i\psi_2}$$

$$c_2 = \frac{\alpha_1 \alpha_2^2}{\cos\psi_1 \cos^2\psi_2} e^{i\psi_1}.$$

The conditions under which equation (23) has real and positive roots are the conditions for existence of a limit cycle. Only the case when $\vartheta_1 = \vartheta_2 = \vartheta_3 = 0$ will be treated further. The conditions for existence of real roots for equation (23) are then

$$1 - 12\frac{\alpha_1}{\alpha_3} > 0. \tag{24}$$

Since $y = Z_1 Z_1^*$, the acceptable roots should be positive. Therefore, in order to get only one acceptable root, i.e., one limit cycle, the product of roots of (23) should be < 0, i.e.,

$$\frac{\alpha_1 \alpha_3}{36\frac{\alpha_1}{\alpha_3} + 9} < 0. \tag{25}$$

Inequalities (24) and (25) are the conditions to obtain a unique limit cycle. These two inequalities are simultaneously satisfied when

$$-\frac{1}{4} < \frac{\alpha_1}{\alpha_3} < 0$$

In order to obtain two limit cycles (the self oscillation, therefore, would be dependent on the initial conditions, i.e., the domain of attraction), the product of roots of (23) and their sum should be positive. These conditions yield

$$\frac{\alpha_1}{4\alpha_1 + \alpha_3} > 0$$

$$\alpha_3(\alpha_3 - 12\alpha_1) > 0$$

$$\alpha_1\alpha_3(12\alpha_1\alpha_2 + \alpha_2\alpha_3) < 0$$

Therefore, here, we have at most two limit cycles. Their stability can be carried out in a straightforward manner, as in the case of two nonlinear oscillators. The algebra is more complicated to be reduced to a simple form, but a parametric discussion is easy to carry out. From a parametric study of the stability of the limit cycles, we have found that when two distinct limit cycles exist they are both unstable. Only the case of one limit cycle has yielded a stable limit cycle. Figures 6a and 6b show the numerical integration of the equations of three nonlinear oscillators for two different sets of initial conditions. The amplitude of the limit cycle is exactly the one acceptable root of equation (23).

The particular case of $|\alpha_1| << |\alpha_2| << |\alpha_3|$ is treated to completion for the initial conditions $B_1(0) = B_2(0) = B_3(0) = 0$. The roots of equation (23) become

$$A_{10} = \pm \frac{1}{\beta}\sqrt{-\alpha_1\alpha_2}$$

$$A_{20} = \frac{\alpha_1}{\beta} \tag{26}$$

$$A_{30} = \pm \frac{3}{\beta}\frac{\alpha_1}{\alpha_3}\sqrt{-\alpha_1\alpha_2}$$

The existence criteria are, therefore, reduced to $\alpha_1\alpha_2 < 0$.

Linearizing the system (1)-(2) near the above solutions and calculating the characteristic polynomial, as for two nonlinear oscillators, yield

$$p(\lambda) = \lambda^3 - \lambda^2(\alpha_2 + \alpha_3) + \lambda(\alpha_2\alpha_3) + 2\alpha_1\alpha_2\alpha_3$$

The stability conditions are then given by applying Lienard criteria

$$\alpha_1\alpha_2\alpha_3 > 0.$$

$$\alpha_2 + \alpha_3 < 0.$$

$$\alpha_2\alpha_3(-\alpha_1 + \alpha_2 - \alpha_3) > 0.$$

The above inequalities yield, by taking into account the existence condition $\alpha_1\alpha_2 < 0$, the following criterion

$$\alpha_1 > 0,\ \alpha_2 < 0,\ \alpha_3 < 0.$$

The direct conclusion here is that all the modes higher than first have to be stable.

1.2. Case of non-zero shift of frequency

In this part, we will consider the case where the coefficients A_i reach the oscillatory behavior $A_i = \delta_i\cos(\nu_i t + \psi_i)$ and B_i reach $B_i = \delta_i\sin(\nu_i t + \psi_i)$ for $t \to \infty$. Substitution into $\eta_i(t) = A_i(t)\sin\omega_i t + B_i(t)\cos\omega_i t$ gives

$$\eta_i(t) = \delta_i \sin((\omega_i + \nu_i)t + \psi_i)$$

Thus, in the limit cycle, the amplitude $\eta_i(t)$ will oscillate with a fundamental frequency of $\omega_i + \nu_i$. The ν_i are yet unknown. The amplitude of the limit cycle as well as its frequency will be determined. The difference from the last section is that here the limit cycle is oscillating with a fundamental frequency different from the fundamental acoustic frequency of the chamber. The shift of frequency is ν_i.

We treat fully the case of two nonlinear oscillators. The case of three oscillators is only integrated numerically in order to confirm the results found for two oscillators. The coefficients A_i and B_i, i=1,2, satisfy then the following system of equations

$$\frac{dA_1}{dt} = \alpha_1 A_1 + \vartheta_1 B_1 - \beta\,(A_1A_2 + B_1B_2) \tag{27}$$

$$\frac{dB_1}{dt} = -\vartheta_1 A_1 + \alpha_1 B_1 + \beta\,(B_1A_2 - A_1B_2) \tag{28}$$

$$\frac{dA_2}{dt} = \alpha_2 A_2 + \vartheta_2 B_2 + \beta\,(A_1^2 - B_1^2) \tag{29}$$

$$\frac{dB_2}{dt} = -\vartheta_2 A_2 + \alpha_2 B_2 + 2\,\beta\,B_1A_1. \tag{30}$$

The ψ_i represent the phase of each oscillator and should be taken into account. However, because the above system is autonomous, one phase is arbitrary, say, $\psi_1 = 0$. Thus, by using the limit expressions of A_i and B_i, equations (27)-(30) reduce to the following system :

$$-\nu_1\delta_1\sin\nu_1 t = \alpha_1\delta_1\cos\nu_1 t + \vartheta_1\delta_1\sin\nu_1 t$$

$$-\beta\,\delta_1\delta_2\cos((\nu_1 - \nu_2)t - \psi_2) \tag{31}$$

$$\nu_1\delta_1\cos\nu_1 t = -\vartheta_1\delta_1\cos\nu_1 t + \alpha_1\delta_1\sin\nu_1 t$$

$$+\beta\,\delta_1\delta_2\sin((\nu_1 - \nu_2)t - \psi_2) \tag{32}$$

$$-\nu_2\delta_2\sin(\nu_2 t + \psi_2) = \alpha_2\delta_2\cos(\nu_2 t + \psi_2)$$

$$+\vartheta_2\delta_2\sin(\nu_2 t + \psi_2) + \beta\,\delta_1^2\cos 2\nu_1 t \tag{33}$$

$$\nu_2\delta_2\cos(\nu_2 t + \psi_2) = -\vartheta_2\delta_2\cos(\nu_2 t + \psi_2)$$

$$+\alpha_2\delta_2\sin(\nu_2 t + \psi_2) + \beta\,\delta_1^2\sin 2\nu_1 t. \tag{34}$$

Multiply equation (31) by $\cos\nu_1 t$, equation (32) by $\sin\nu_1 t$ and add the results, to find

$$\alpha_1\delta_1 - \beta\,\delta_1\,\delta_2\cos((2\nu_1 - \nu_2)t - \psi_2) = 0.$$

This equation should be satisfied at any (large) time, therefore

$$\nu_2 = 2\,\nu_1$$

and

$$\alpha_1 - \beta\delta_2\cos\psi_2 = 0. \tag{35}$$

The values of ψ_2 and δ_2 have yet to be determined. Now, multiply equation (31) by $\sin\nu_1 t$, equation (32) by $\cos\nu_1 t$ and subtract the results to find

$$-\nu_1 = \vartheta_1 - \beta\delta_2\sin((2\nu_1 - \nu_2)t - \psi_2)$$

Then, with $2\nu_1 = \nu_2$,

$$-\nu_1 = \vartheta_1 + \beta\delta_2\sin\psi_2 \tag{36}$$

Equations (35) and (36) yield

$$\tan\psi_2 = -\left(\frac{\vartheta_1 + \nu_1}{\alpha_1}\right) \tag{37}$$

A second relation is obtained by multiplying equation (33) by $\cos(\nu_2 t + \psi_2)$, equation (34) by $\sin(\nu_2 t + \psi_2)$ and adding the results to find

$$\alpha_2\delta_2 + \beta\,\delta_1^2\cos((2\nu_1 - \nu_2)t - \psi_2) = 0.$$

This equation should be satisfied at any (large) time, and, giving $\nu_2 = 2\,\nu_1$ again,

$$\alpha_2\delta_2 + \beta\delta_1^2\cos\psi_2 = 0. \qquad (38)$$

Finally, multiply equation (33) by $\sin(\nu_1 t + \psi_2)$, equation (34) by $\cos(\nu_2 t + \psi_2)$, and subtract the results to find

$$-\nu_2\delta_2 = \vartheta_2\delta_2 - \beta\delta_1^2\sin(\,(2\nu_1 - \nu_2)\,t - \psi_2\,)$$

This becomes, with $2\nu_1 = \nu_2$,

$$\delta_2(\nu_2 + \vartheta_2) + \beta\delta_1^2\sin\psi_2 = 0. \qquad (39)$$

Equations (38) and (39) then imply

$$\tan\psi_2 = \left(\frac{\vartheta_2 + \nu_2}{\alpha_2}\right) \qquad (40)$$

Equations (37) and (40) yield the following expression for the shift of frequency

$$\nu_1 = -\frac{\alpha_2\vartheta_1 + \vartheta_2\alpha_1}{2\alpha_1 - \alpha_2} \qquad (41)$$

Therefore, the shift of frequency is zero when $\alpha_2\vartheta_1 + \vartheta_2\alpha_1 = 0$. That is exactly the condition (13) for zero shift of frequency. Using the result (41), equations (35) give

$$\delta_2 = \frac{\alpha_1}{\beta}\left(1 + \left(\frac{2\vartheta_1 - \vartheta_2}{2\alpha_1 + \alpha_2}\right)^2\right)^{\frac{1}{2}} \qquad (42)$$

Equation (38) then yields

$$\delta_1^2 = -\frac{\alpha_1\alpha_2}{\beta^2}\left(1 + \left(\frac{2\vartheta_1 - \vartheta_2}{2\alpha_1 + \alpha_2}\right)^2\right) \qquad (43)$$

Equations (42) and (43) show that the amplitudes of the two modes have increased when $\vartheta_1 \neq 0$., in comparison with the amplitudes of the two modes in the past section when $\vartheta_1 = 0$. Moreover, for existence of solutions, we should have, as before,

$$\alpha_1\alpha_2 < 0.$$

To verify the analytical results, Figures 7a and 7b show the numerical solutions of the system (27)-(30) of ordinary differential equations for different initial conditions. The limiting amplitudes have exactly the same values given by the formulas (42) and (43).

By studying the stability of the limit cycle, the direction of energy flow can be handled in the same manner as for the case of zero shift of frequency. The treatment is more complicated since the linearization of the system of nonlinear oscillators leads to a *parametric* linear system. An approach is presented in reference [16] to solve this linear system. The results confirm the conclusions reached in the case of zero-shift of frequency regarding the influence of $(\vartheta_1, \vartheta_2)$ on the stability of the limit cycle.

In order to enhance our conclusion that the stability conditions of the limit cycle for the case $\vartheta_1 = 0$ are *sufficient* for the stability of the limit cycle for the case $\vartheta_1 \neq 0$, system (1)-(2) is integrated for three modes with two arbitrary sets of ϑ_1 but for the same set of α_1 used in Figures 6. Figures 8a and 8b show that the limit cycle is indeed stable, independently of the ϑ_1. This enhances the conclusion reached above for two nonlinear oscillators.

1.3. Comparison with numerical solutions and experimental results

First, we will compare the results of this analysis with the numerical solutions reported in reference [7]. Second, comparison will be made with some experimental results reported in reference [9].

1.3.1. Comparison with some numerical results .

In [7], Levine and Baum used a numerical technique based on a finite difference scheme to solve the longitudinal waves in the combustion chamber of a solid propellant rocket motor. Figures 9 show two of their results. Figure 9a shows the waveform of the pressure oscillations for a flow without particles, while Figure 9b is for flow with 2.5 μ particles. The initial disturbance contains only the fundamental mode but the final waveform (large time) contains higher harmonics. The fundamental mode grows initially in time, indicating that the first mode is unstable and with a growth rate α_1 given approximately by the initial exponential growth rate of the pressure. The amplitude of the second harmonic will be used as a basis for comparing our theoretical results and the numerical results in these Figures. This amplitude can be determined from the numerical data by a Fourier analysis of the waveform. The growth rate of the first mode can be determined from the variation of the amplitude at the initial growth of the wave. In their numerical results[7], the relative energy density of the first three modes were respectively 0.813, 0.103, and 0.033 for the case in Figure 9a, and 0.811, 0.102, and 0.038 for the case in Figure 9b. These numbers show that the approximation $|\alpha_1| << |\alpha_2| << |\alpha_3|$ is valid here. On the other hand, the frequency shift is zero in Figure 9a and very small in Figure 9b, indicating that it is safe to assume that $\vartheta_1 = 0$. Therefore, the amplitude of the second harmonic, given approximately, equation (26), by

$$A_{20} = \frac{\alpha_1}{\beta}$$

can indeed be a criterion for comparison. Table 1 shows a comparison of the value of the spectral density of the second mode (proportional to the square of the amplitude) between our analysis and the results reported in [7]. Good agreement is found.

Since here the first mode is unstable and the second and third modes, we think, are stable, the energy of the wave is flowing from the first mode to the second and the third mode

Table 1 : Comparison between Analysis and Numerical Results of [7]

	α_1 s^{-1}	Spectral density of second mode Analysis	Numerical [7]	Error %
Figure 9a	61.31	0.1215	0.103	17.9%
Figure 9b	48.26	0.077	0.102	24.3%

1.3.2. Comparison with some experimental results .

In the experiments reported by Beckstead et al [9], they carried out a series of experiments on the performance of T-Burners. In particular, they changed the combustion area of the solid propellant and they determined, at the same time, the growth α_1 of the first mode and the final amplitude of the limit cycle. But, from our analysis, the final amplitude is given by

$$A = \sqrt{(A_1^2 + A_2^2)} = \frac{1}{\beta}\sqrt{\alpha_1(\alpha_1 - \alpha_2)} \qquad (44)$$

by limiting the number of modes to two. Considering the fact that for practical problems the damping is approximately independent of the combustion area and the growth rate of the first mode is small compared to the damping rate of the second mode, it is safe to assume from our analytical results (44) that the amplitude varies as the square root of the growth rate of the first mode when the combustion area changes. This criterion is used to compare with the experiments in [9]. Figure 10 shows the result of the comparison. A fairly good agreement is found.

2. TRIGGERING OF PRESSURE OSCILLATIONS

The above analysis is limited to the determination of the limit cycle when the system is linearly unstable, i.e. one or more modes is linearly unstable. It cannot predict the nonlinear instability, or triggering. In fact, system (1)-(2) yields

$$\frac{1}{2}\frac{d}{dt}\sum_{i=1}^{\infty}(A_i^2 + B_i^2) = \sum_{i=1}^{\infty}\alpha_i(A_i^2 + B_i^2)$$

Therefore, the nonlinearity disappears when we calculate the rate of change of the energy of the wave. For a linearly stable system, all the α_i are negative and the energy of the wave decays in time, whatever the initial conditions are.

The analysis should be changed in order to explain how a linearly stable system can be pulsed into instability; i.e., for small initial conditions the system is stable, but for large initial conditions the wave amplitude will grow in time, leveling off toward a non-trivial limit cycle. One basic assumption in the above analysis is that the boundary conditions are linear. The nonlinearity represents only second order nonlinear gasdynamics. Here, we will assume that the boundary conditions are nonlinear. Only the nonlinearity of the combustion response and particle attenuation, along with the gasdynamics nonlinearity, will be accomodated. The nonlinearity of the nozzle response can be incorporated without further difficulty.

Using a nonlinear combustion response leads ultimately to a system of nonlinear oscillators. The point is to see when a system of nonlinear oscillators can predict triggering. The first step is obviously to start with a simple nonlinear differential equation of the form

$$\frac{dA}{dt} = \alpha A + b A^2 + c A^3$$

A discussion of the phase plane of this equation shows clearly that in order to get triggering to a non-trivial stable limit cycle, it is necessary and sufficient that

$$b \neq 0, \quad c \neq 0 \quad \text{and} \quad \frac{c}{\alpha} > 0. \qquad (45)$$

The central question now is : are these conditions still required to get a triggering phenomenon for a *system* of nonlinear oscillators?.

To answer this question, we studied first a system of two ordinary differential equations

$$\frac{dA_1}{dt} = \alpha_1 A_1 - \beta_1 A_1 A_2$$

$$\frac{dA_2}{dt} = \alpha_2 A_2 + \beta_2 A_1^2$$

Ignoring "out-of-phase" components B_1 and B_2, this system corresponds to a second order nonlinear pressure combustion response of the form

$$\frac{m'}{p'} = \mu + b\,p' \text{ or } \mu + b\,\frac{\partial p'}{\partial t}$$

where μ is the linear combustion response and b is an arbitrary coefficient. For α_1 and α_2 both negative, we found that this system did not yield a stable non-trivial limit cycle. Therefore, such a form of the combustion response cannot predict triggering.

Second, we treated the system of two ordinary differential equations

$$\frac{dA_1}{dt} = \alpha_1 A_1 - \beta A_1 A_2 + c_1 A_1^2$$

$$\frac{dA_2}{dt} = \alpha_2 A_2 + \beta A_1^2$$

Ignoring "out-of-phase" components, this system corresponds to a second order nonlinear pressure combustion response of the form

$$\frac{m'}{p'} = \mu + c \left| \frac{\partial p'}{\partial t} \right|$$

where c is an arbitrary coefficient. This form may represent a second order nonlinear velocity coupling. Triggering, in the sense of a stable non-trivial limit cycle, was found. Unlike the case in Section 1, the stability of the limit cycle here depends also on the *nonlinear* coefficients. Figure 11 shows the existence of triggering for a particular set of coefficients α_1, α_2, β, and c_1. From this graph, it is clearly seen that for a small (0.05) initial disturbance the wave decays in time but for a large (0.18) initial disturbance the wave grows to a non-trivial limit cycle.

Third, we examined the third order system

$$\frac{dA_1}{dt} = \alpha_1 A_1 - \beta_1 A_1 A_2 + d_1 A_1^3$$

$$\frac{dA_2}{dt} = \alpha_2 A_2 + \beta_2 A_1^2 + d_2 A_1^2 A_2$$

This corresponds to a combustion response of the form

$$\frac{m'}{p'} = \mu + b_1 p' + f_1 \frac{\partial p'}{\partial t} + b_2 p'^2 + f_2 p' \frac{\partial p'}{\partial t} + h_2 \left(\frac{\partial p'}{\partial t} \right)^2$$

where b_1, f_1, b_2, f_2, and h_2 are arbitrary coefficients. The coefficients β_1 and β_2 are dependent on both the nonlinear gasdynamics and the nonlinear combustion response. The coefficients d_1 and d_2 depend only on the nonlinear combustion response. Triggering does occur. The stability of the limit cycle depends on the nonlinear as well as on the linear coefficients. Figure 12 shows the existence of triggering for a particular set of coefficients. The triggering phenomenon here is quite similar to the one shown on Figure 11.

From the above results, one concludes that triggering seems to be due mainly to the energy exchange among modes and either to a *second* order nonlinear velocity coupling or to a *third* order nonlinear pressure coupling.

In order to obtain a model which can represent some physical phenomenon, both velocity and pressure couplings should be present. We expanded the combustion response to *third* order in the pressure amplitude

$$\frac{m'}{p'} = \mu + b_1 \left| \frac{\partial p'}{\partial t} \right| + b_2 p'^2 + f_2 p' \frac{\partial p'}{\partial t} + h_2 \left(\frac{\partial p'}{\partial t} \right)^2 \qquad (46)$$

This form includes both second order nonlinear velocity and third order nonlinear pressure couplings. Triggering does occur. For one mode, conditions (45) should be satisfied. Therefore, whether one mode is sufficient to predict triggering depends on the various parameters in (46), i.e. on the model for the combustion response. On the other hand, we found that h_2 was the only important coefficient among third order term coefficients. Later in the analysis, h_2 will be found to be associated with the time-lag in the combustion response.

To make the analysis more practical, we treat only the triggering of pressure oscillations in solid propellant rockets. However, the analysis yields results which can be generalized to other types of systems.

A detailed formulation for triggering is presented below. From the conservation equations of one-dimensional flow in solid propellant rocket motors, the existence of triggering for pressure oscillations in combustion chambers is proved. For a given set of parameters, one stable limit cycle is shown to exist. The main reason for existence and stability is the equilibrium among velocity coupling, nonlinear driving of the combustion (mostly due to the time lag between the pressure and the combustion response), nonlinear losses (particles, etc.) and the energy exchange among the acoustic modes of the chamber. The presence of nonlinear losses (particles, etc.) is not necessary as long as velocity coupling is taken into account.

An application to some experimental results, reported in [17], is carried out. Good agreement is found. Then we apply the analysis to some numerical solutions reported in [18].

2.1. Preliminary

In the theory of deflagration of solid propellant, a simple model[11] relating the propellant burning rate to the pressure is given by

$$r(t) = r_0(t)(1 + \frac{\psi\, n\, \kappa}{r_0^3(t)} \frac{dr_0(t)}{dt}) \qquad (47)$$

where r_0 is the steady state burning rate: $r_0 = ap^n$, ψ is a constant having a value close to unity and is dependent on the propellant and the combustion model; n is the burning rate exponent; and κ is the thermal diffusivity of the solid propellant.

On the other hand, an imaginary part in the combustion response of the solid propellant to pressure oscillation represents a time-lag. Following a similar reasoning, a nonlinear combustion model should reflect a similar behavior, i.e., the nonlinear combustion response should reflect a time-lag. The time-lag concept in combustion chamber was first introduced by Crocco and Cheng[12] for concentrated combustion and by Cheng[13] for the specific problem of solid propellant rockets. Their attention was focused on the abnormal pressure peaks in rockets and their analysis was solely linear. To interpret the triggering of pressure oscillations in liquid propellant rockets, Sirignano[14] used a shock wave model with a time-lag in the propellant combustion. His analysis predicted triggering but did not give either the threshold value or the final amplitude. Recognizing these shortcomings, Mitchell[15] calculated numerically the final amplitude, after tedious algebraic manipulations. It is difficult to interpret the relative importance of the different physical processes. The point here is to present a simple model which can be used to predict, in a simple way, both the threshold and the final amplitudes.

2.2. Analysis

We are looking for combustion response of the form (46). The following representation of the burning rate

$$r(t) = r_0(t-\tau)(1 + \frac{\psi\, n\, \kappa}{r_0^3(t-\tau)} \frac{dr_0(t-\tau)}{dt} + g\,|u'|\,) \qquad (48)$$

yields, after expansion in the pressure amplitude, the desired form (46). The term $g\,|u'|$ may represent velocity coupling.

In the conservation equations of one-dimensional flow in cylindrical solid propellant rockets we expand the pressure, temperature, and velocity,

$$T = \bar{T} + \varepsilon T', \quad p = \bar{p} + \varepsilon p', \quad u = \bar{u} + \varepsilon u'$$

where $\bar{T}$, $\bar{p}$, $\bar{u}$ correspond to the steady state conditions. The unsteady pressure and velocity are written as expansions[4] in two modes only:

$$p' = \eta_1(t)\cos\omega x + \eta_2(t)\cos 2\omega x$$

$$u' = -\frac{\dot{\eta}_1(t)}{\gamma\omega}\sin\omega x - \frac{\dot{\eta}_2(t)}{2\gamma\omega}\sin 2\omega x\,,$$

We assume η_1 and η_2 to have the forms

$$\eta_1 = A_1(t)\sin\omega t, \quad \eta_2 = A_2(t)\sin 2\omega t \qquad (49)$$

The expansion presented in equation (49) implies that the initial conditions contain only the rate of change of the pressure at t=0. Also it is assumed that the phases, i.e. the B_i, are not important. In reference [16], it is shown that in the expansion to third order in the pressure amplitude, the third order terms in the the expansion of the nonlinear gasdynamics term $\rho u \frac{\partial u}{\partial x}$ contain only coupling terms between the A_i and B_i. Therefore, neglecting the B_i implies neglecting the third order contribution of the nonlinear gasdynamics. The effect of this assumption has not yet been assessed. However, experimental data[17] favor this assumption in the sense that triggering is amplitude dependent. One direct result is that, for two modes, the number of nonlinear differential equations is reduced to 2, thus making the discussion of stability and existence of the triggering limit easy to handle. One direct conclusion from assumption (49) is that the initial conditions presented in the results in the next section correspond, not to the amplitude of the pulse, but rather to the initial rate of change of pressure.

The approximate analysis[4, 16] leads to the following system of ordinary differential equations for the A_i, i = 1,2,

$$\frac{dA_1}{dt} = \alpha_1 A_1 - \beta A_1 A_2 + G_1 A_1^2 + c_1\omega^2 A_1^3 + d_1\omega^2 A_1 A_2^2 \qquad (50a)$$

$$\frac{dA_2}{dt} = \alpha_2 A_2 + \beta A_1^2 + G_2 A_2^2 + c_2\omega^2 A_2^3 + d_2\omega^2 A_1^2 A_2 \qquad (50b)$$

Here, only the coefficient β represents the nonlinear gasdynamics. The coefficients c_i, d_i, i = 1,2, are functions of ratio γ of the specific heats, the burning rate exponent n, and the area ratio and they are proportional to the coefficient h_2 in (46). Moreover, the coefficient c_1 is found[16] to be positive. Since α_1 is negative, $\frac{c_1}{\alpha_1}$ is negative. Therefore, conditions (45) are not satisfied for the first mode. However, the coupling between A_1 and A_2 will allow, as we will see in the applications, triggering to occur. The conclusion here is that, for solid propellant rockets and with the model (48) for the combustion response, we need at least two

modes to predict triggering.

The coefficient h_2 is found, by expanding the burning rate expression in the pressure amplitude, to be proportional to the time-lag τ. The coefficient G_1 and G_2 represent either nonlinear velocity coupling or nonlinear particle losses. Reference [16] contains the details of the calculation leading to equations (50), along with the details for the expressions of c_1 and d_1.

2.3. Determination of the limit cycle

In the limit cycle, equations (50) become

$$\alpha_1 A_1 - \beta A_1 A_2 + G_1 A_1^2 + c_1 \omega^2 A_1^3 + d_1 \omega_2 A_1 A_2^2 = 0. \qquad (51a)$$

$$\alpha_2 A_2 + \beta A_1^2 + G_2 A_2^2 + c_2 \omega^2 A_2^3 + d_2 \omega^2 A_1^2 A_2 = 0 \qquad (51b)$$

Equation (51b) yields

$$A_1^2 = \frac{-\alpha_2 A_2 + G A_2^2 - c_2 \omega^2 A_2^3}{\beta + d_2 \omega^2 A_2} \qquad (52)$$

Equations (51a) and (52) then give

$$y^6 + e_5 y^5 + e_4 y^4 + e_3 y^3 + e_2 y^2 + e_1 y + e_0 = 0 \qquad (53)$$

where $y = A_2$ and e_i are functions of the different parameters in equations (50). The different limit cycles are found by solving equation (53). The acceptable solutions are the real roots of (53) which give a positive value to the right-hand-side of equation (52).

The stability of a given solution (A_{10}, A_{20}) is handled by linearizing the system (50) near this solution and by calculating the eigenvalues of the obtained linear system, as we have done before for two and three oscillators.

2.4. Application

In the following, we apply the above analysis to some experimental results reported in [17]. The point is to show that the analysis can predict triggering. Then, we apply the analysis to some numerical solutions reported in [18]. The purpose there is to show that we can replace velocity coupling by nonlinear particle losses and still predict triggering.

2.4.1. Application to some experimental results .

In order to show that the above theory can indeed predict triggering, Equations (50) are first applied to the series MSA-19 to 26 of the experiments in [17] on the triggering phenomenon in subscale solid propellant motors, shown on Figure 13a. In these experiments, a smokeless cylindrical solid propellant rocket motor was pulsed into instability and both the threshold value and the final amplitude were recorded. No solid particles were present in the flow; thus the coefficients G_1 and G_2 may represent only velocity coupling.

Figure 13b shows the numerical integration of equations (50) to a particular set of experiments in [17]. It is clearly seen from this figure that triggering can indeed be predicted. A stable non-trivial limit cycle is reached for the pressure oscillations in a linearly stable (α_1 and α_2 are negative) system. The values of the parameters shown on Figure 13a are chosen such that the limit cycle amplitude is close to the experimental one. G_1 is taken to be positive (driving term) and G_2 to be negative (damping term). It is worth noticing here that the value 2.10^{-4}s of the time-lag used in the comparison lies well in the range of values of time-lag reported in [13]. The values -1.0 and -50.0 for α_1 and α_2 lie in the practical range of linear decay rates. No physical explanation has been found for the coefficients G_1 and G_2 apart from the association with velocity coupling.

Figure 13c shows the triggering threshold. When the initial pulse amplitude is below certain value the wave decays. The low value of 0.004 represents the initial rate of change of the pressure and not the pulse amplitude. The amplitude of the pulse is deduced from the geometry and the location of the pulser, and the duration of the pulse. For practical pulsers, this rate corresponds, as it is the case of this application, to approximately 8% of the mean pressure.

Table 2 shows a comparison between the theoretical and the experimental results. Good agreement is found in predicting both the limit cycle amplitude and triggering threshold.

Table 2 : Comparison between Analysis and Experimental Results of [17]

	Analysis	Experiment [17]	Error%
Limiting Amplitude	0.106	0.122	14%
Pulse Amplitude (psi)	86.8	108.	19.6%

The parametric study of the triggering phenomenon is carried out by varying the values of the parameters α_1, α_2, τ, G_1, and G_2. It is found that triggering is very sensitive to the decay rate α_1 of the first mode. The lower is the value $|\alpha_1|$, the higher is the limit cycle amplitude. If both G_1 and G_2 vanish, then the triggering phenomenon disappears.

Also from the parametric study, we have found that always the stable limit cycle is unique. This is found for a wide range of the parameters. For a given set of parameters, many limit cycles can exist but at most one is stable.

2.4.2. Application to some numerical solutions .

In reference [18], a numerical integration of the

conservation equations in a one-dimensional solid propellant rocket is reported. The combustion model used did not include velocity coupling. However, particle attenuation was accounted for. The point here is not to apply exactly our analysis to the particular problem treated in [18] but rather to show that our model can predict triggering in the absence of velocity coupling if we include the nonlinear particle losses.

Equations (50) are applied to the case of the cylindrical rocket shown on Figure 14a. In this case, both G_1 and G_2 are negative. They correspond[10] to the second order nonlinear particle losses, with $G_2 = 8G_1$.

In Figure 14b, it is clearly seen that triggering can indeed be predicted without the inclusion of velocity coupling. A stable limit cycle, as before, is unique. Figure 14c shows the triggering threshold for pressure oscillations. Figure 14d shows the sensitivity of triggering to the decay rate α_1 of the first mode. In this figure, all the parameters in Figure 14a remain the same except that α_1 has now the value of -3 instead of -1. Even for a very high initial rate of change of pressure of 0.25, the wave decays in time.

CONCLUSION

In this paper, we have shown, following a second order expansion in the pressure amplitude, analytical expressions for the amplitude, and the conditions for existence and stability of limit cycles of pressure oscillations in combustion chambers. The limit cycle seems to be unique. Under very special conditions, the initial conditions affect the stability of the limit cycle. The imaginary parts of the linear responses of the different processes strongly influence the stability criteria and the amplitude of the limit cycle. They affect the exchange of energy among modes.

A model of the combustion response including both a *second* order nonlinear velocity coupling *and* energy exchange among modes predicts triggering. A model including a *third* order nonlinear pressure response *and* energy exchange among modes can predict triggering. The triggering phenomenon in solid propellant rockets seems to be due mainly to three factors : second order nonlinear velocity coupling , third order nonlinear pressure coupling in the combustion response, and energy exchange among modes. However, in principle, second order nonlinear particle damping can replace the velocity coupling as a factor for triggering. The nonlinear pressure coupling is due mainly to the time-lag. A stable non-trivial limit cycle seems to be unique.

The results reported in this analysis can be obtained using a regular perturbation technique[16] in the pressure amplitude.

AKNOWLEDGMENTS

This work was supported by the California Institute of Technology, by the Air Force Office of Scientific Research, Grant No. AFOSR-80-0265, and by the Naval Weapons Center, Contract N 60530-82-C-0137.

APPENDIX A

In this appendix we will show that the limit cycle can have, under certain conditions, only two forms. To fix ideas, we treat two modes only and we deal with the pressure at a given location, say, x=0. The pressure has then the following expression

$$p' = \eta_1(t) + \eta_2(t)$$

Since we are looking for periodic solutions, the pressure should be periodic and with fundamental frequency, say, $\omega + \nu$. Now, expand the pressure into its Fourier components

$$p' = a_1\sin((\omega + \nu)t + \psi_1)$$

$$+ a_2\sin(2(\omega + \nu)t + \psi_2) + \text{etc.} \qquad (A1)$$

On the other hand

$$p' = A_1(t)\sin\omega t + B_1(t)\cos\omega t$$

$$+ A_2(t)\sin 2\omega t + B_2(t)\cos 2\omega t \qquad (A2)$$

Equating equations (A1) and (A2) yields

$$\sin\omega t(A_1(t) - a_1\cos(\nu t + \psi_1))$$

$$+ \cos\omega t(B_1(t) - a_1\sin(\nu t + \psi_1))$$

$$+ \sin 2\omega t(A_2(t) - a_2\cos(2\nu t + \psi_2))$$

$$+ \cos 2\omega t(B_2(t) - a_2\sin(2\nu t + \psi_2)) = 0. \qquad (A3)$$

Two direct solutions of (A3) are

$$A_1(t) = \text{constant}, \quad \nu = 0.$$

and

$$A_1(t) = a_1\sin(\nu t + \psi_1) \qquad (A4)$$

This is the origin of the two cases treated in the main text.

Now assume that $A_1(t)$, etc., oscillate with a frequency much smaller than ω, and the shift of frequency ν is small compared to ω. Multiply (A3) by $\sin\omega t$ and integrate over one period, keeping in mind that the coefficient of $\sin\omega t$ remains approximately constant. The direct result is that this coefficient should vanish in order for (A3) to be satisfied:

$$A_1(t) - a_1\sin(\nu t + \psi_1) = 0$$

That is exactly equation (A4). Therefore, under the assumption of a very small shift of frequency, we have only the cases treated in the main text. It is worth noticing here that this assumption was essential in applying the method of averaging in reference [4].

If this assumption is not satisfied, then a number of cases are possible. For example

$$A_1(t) = a_1\cos(\nu t + \psi_1) + \cos\omega t$$

$$B_1(t) = a_1\sin(\nu t + \psi_1) - \sin\omega t, \text{ etc.}$$

are solutions of equation (A3).

REFERENCES

1. " *T-Burner Manual*," edited by Culick, F. E. C., CPIA pub. 191, Nov. 1969.

2. Stoker, J. J. " *Nonlinear Vibration in Mechanical and Electrical Systems* ," Interscience Publishers Inc., New York, 1950, pp. 119-128.

3. Culick, F. E. C. " Nonlinear Growth and Limiting Amplitude of Acoustic Oscillations in Combustion Chambers," *Combustion Science and Technology*, 1971, Vol. 3, pp. 1-16.

4. Culick, F. E. C. " Nonlinear Behavior of Acoustic Waves in Combustion Chambers," *Acta Astronautica*, Vol. 3 , No. 9, Sept. 1976.

5. Jensen, R. C. and Beckstead, M. W. " Nonlinear Mechanisms of Solid Propellant Instabilities," *AIAA* paper 73-1297, November 1973.

6. Culick, F. E. C. and Levine, J. N." Comparison of Approximate and Numerical Analysis of Nonlinear Combustion Instabilities," *AIAA* paper 74-201, January 1974.

7. Levine, J. N. and Baum, J. D." A numerical Study of Nonlinear Instabilities in Solid Rockets Motors," *AIAA* paper 81-1524, July 1981.

8. Gantmacher, F. R. "*The Theory of Matrices*," Chelsea Publishing Company, New York, 1960.

9. Beckstead, M. W., Bennion, D. U., Butcher, A. G., and Peterson, N. L. " *Variable Area T-Burner Investgation*," AFRPL-TR-72-85.

10. Jensen, R. C. and Beckstead, M. W. " Limiting Amplitude Analysis ," Hercules Inc., Utah, Bacchus Works, July 1973.

11. von Elbe, G. " Solid Propellant Ignition and Response of Combustion to Pressure Transients," *AIAA* paper 66-668.

12. Crocco, L. and Cheng, S. I. " High Frequency Combustion Instability in Rockets Motors with Concentrated Combustion," *Journal of The American Rocket Society*, Vol. 23, 1953, pp. 301-303.

13. Cheng, S. I. " High Frequency Combustion Instability in Solid Propellant Rockets," *Journal of The American Rocket Society*, Vol. 24, 1954, pp. 27-32.

14. Sirignano, W.A " Theoretical Stvdy of Nonlinear Combustion Instabilities : Longitudinal Mode," Technical Report No. 677, Department of Aerospace and Mechanical Sciences, Princeton University, March 1964.

15. Mitchell, C. E." Axial Mode Shock Wave Combustion Instability in Liquid Propellant Rocket Engines," Ph. D. Thesis, Princeton University, July 1967.

16. Awad, E. " Nonlinear Instabilities in Combustion Chambers," Ph. D. Thesis, California Institute of Technology, (To be published).

17. Micheli, P. L. et al " Experiments on Subscale Tactical Solid Propellant Rockets," Aerojet Corporation, Sacramento, CA, 1982. (To be published).

18. Kooker, D. E. and Zinn, B. T. " Triggering Axial Instabilities in Solid Rockets: Numerical Predictions." *AIAA* paper 73-1298.

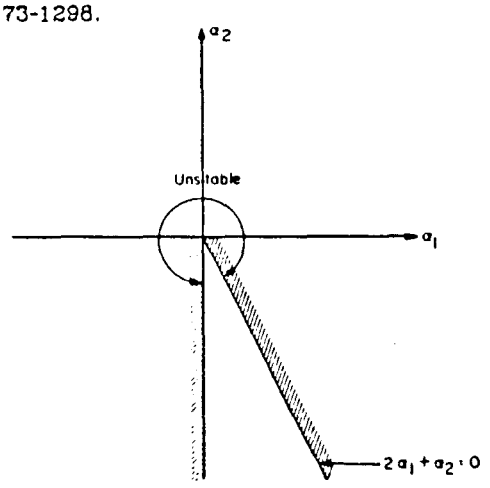

Fig. 1 Domaine of stability for two nonlinear oscillators

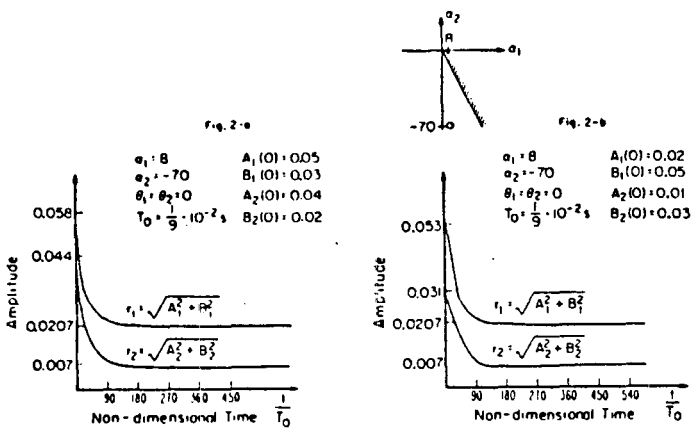

Fig. 2 The non-influence of the initial conditions on the limit cycle amplitude

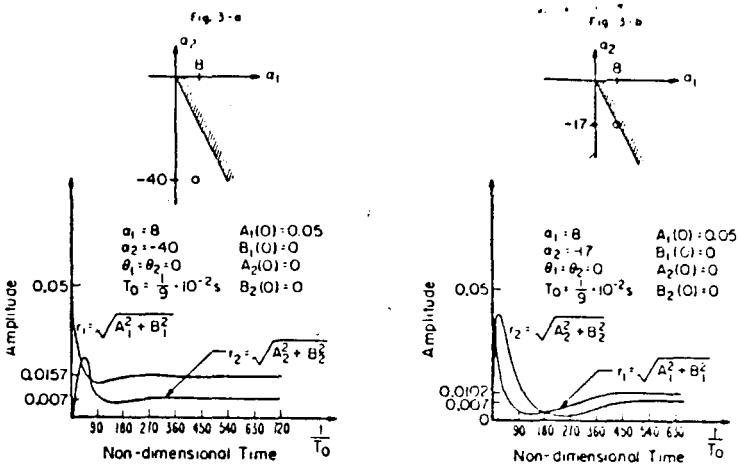

Fig. 3 Influence of the dumping rate a_2 on the speed of reaching the limit cycle.

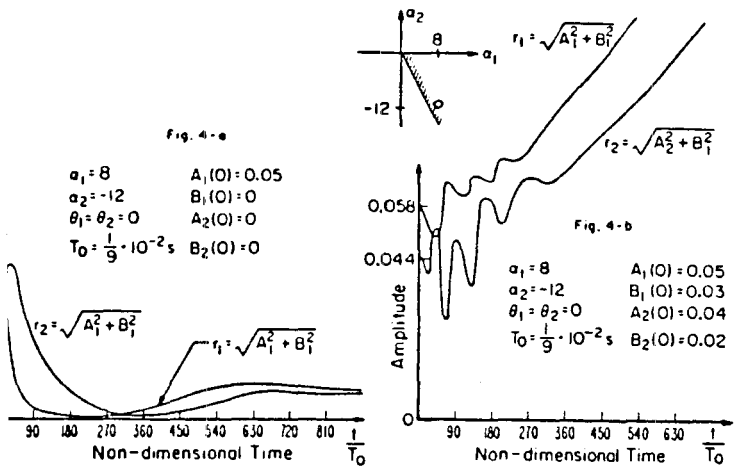

Fig. 4 Influence of the initial conditions on the stability criteria.

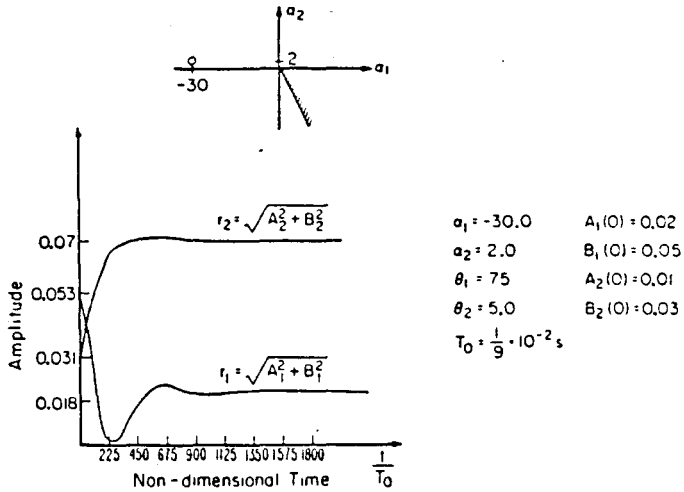

Fig. 5 Influence of the imaginary part on the stability conditions. Conditions (I-16)-(I-18) are not satisfied. Condition (I-22) is satisfied.

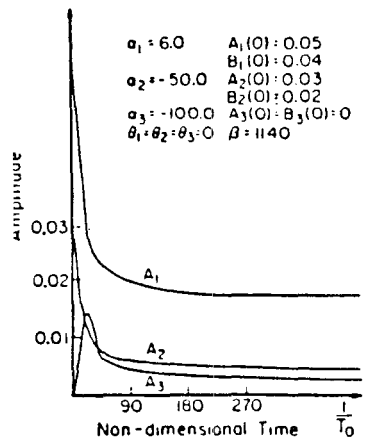

Fig. 6a

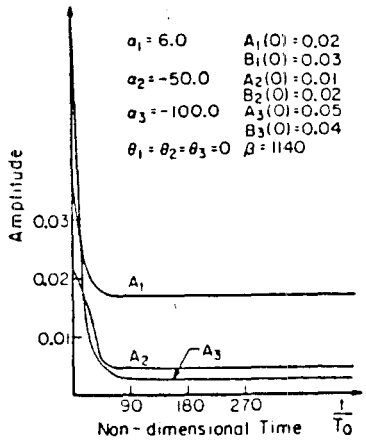

Fig. 6b

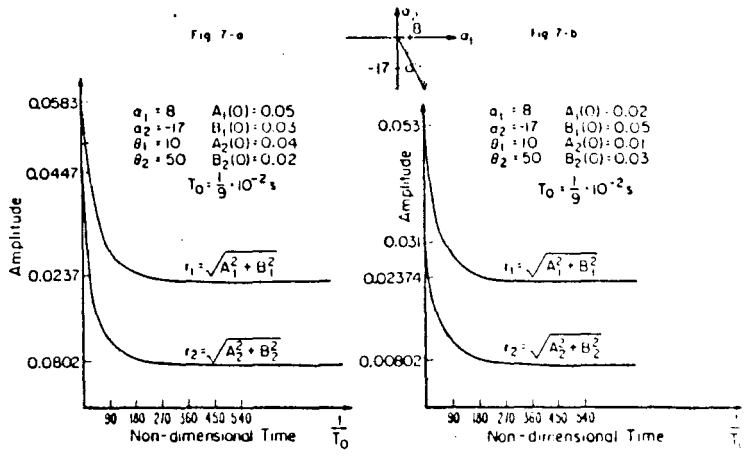

Fig. 7 Influence of the θ_1 on the increase of the amplitude of the limit cycle. Compare these results with those of Figure 2.

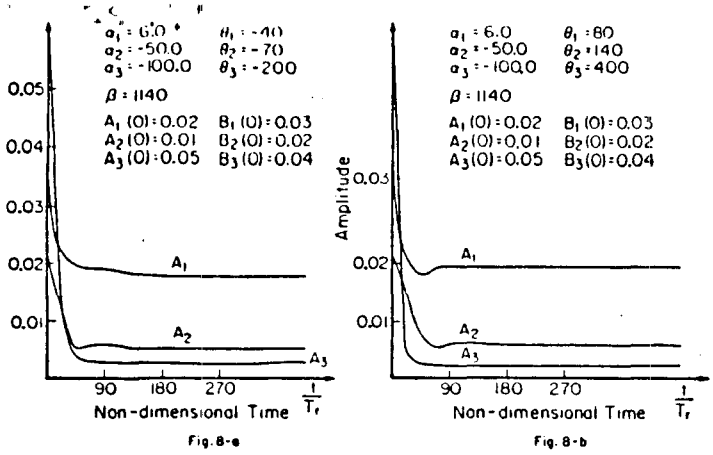

Fig. 8-a Fig. 8-b

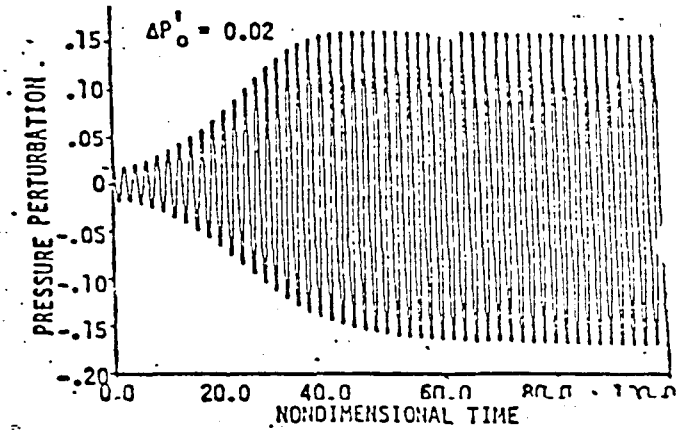

Fig. 9a Time Evolution of Pressure Oscillations At the head End of a Motor (No Particles). Reference [7].

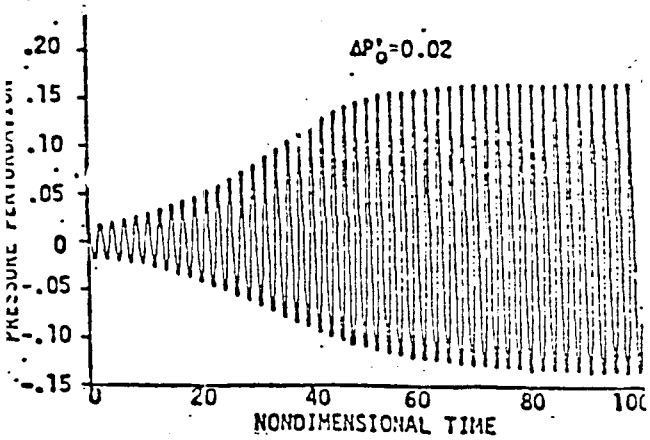

Fig. 9b Time Evolution of Pressure Oscillations At the head End of a Motor (15%, 2 Micron Particles). Reference [7].

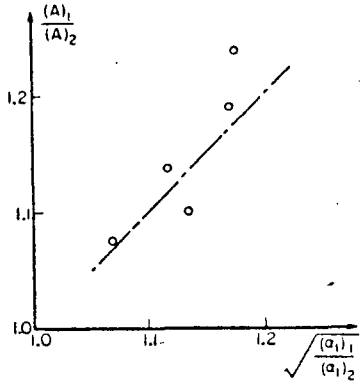

Fig. 10 Comparison of the analytical results with the experimental ones given in reference [8]. The straight line represents approximate analytical result.

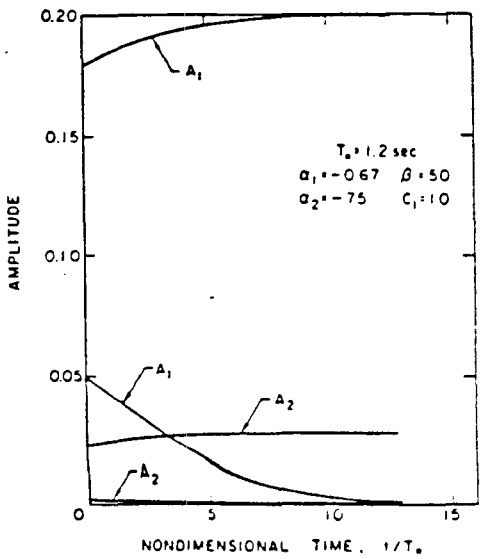

11 Proof of the ability of second order nonlinear velocity coupling to predict triggering.

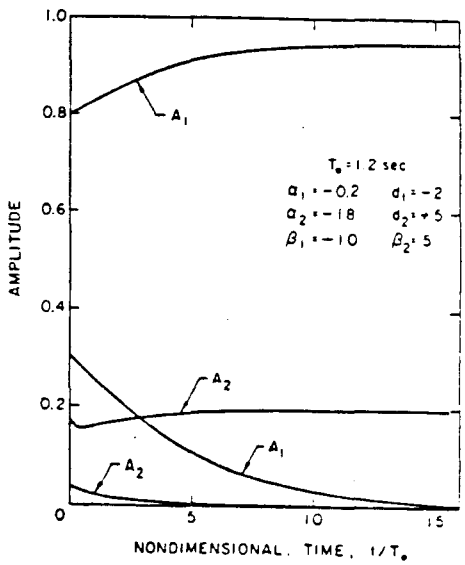

Fig. 12 Proof of the ability of third order nonlinear pressure coupling predict triggering.

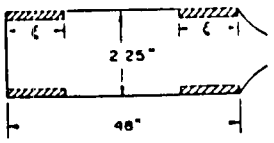

$\xi = 10"$	$a_1 = -0.75\ s^{-1}$	$n = 0.43$
$P_s = 1500$ psi	$a_2 = -50\ s^{-1}$	$\gamma = 1.23$
$G_1 = 240$	$G_2 = -2400\ s^{-1}$	$K = 2.7\ 10^{-7} m^2 s^{-1}$
$N = 400$ Hz	$\tau = 2\ 10^{-4} s$	$\rho s = 1.7\ 10^3 Kg m^{-3}$
$T_r = \frac{1}{N}$	$\omega = 2\pi N$	$a = 0.01\ ms^{-1}$

Fig. 13a

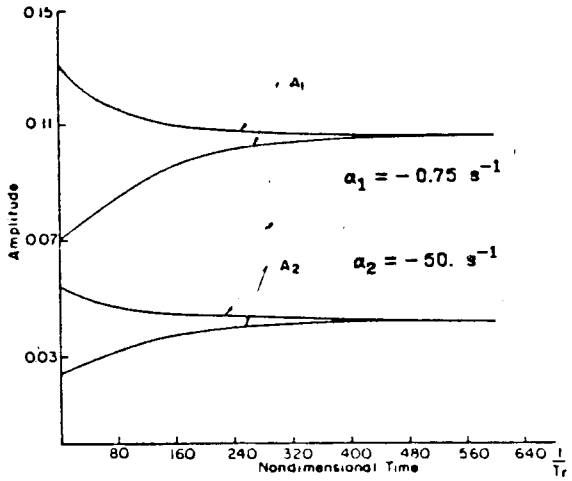

Fig. 13b EXISTENCE OF A NONTRIVIAL LIMIT CYCLE

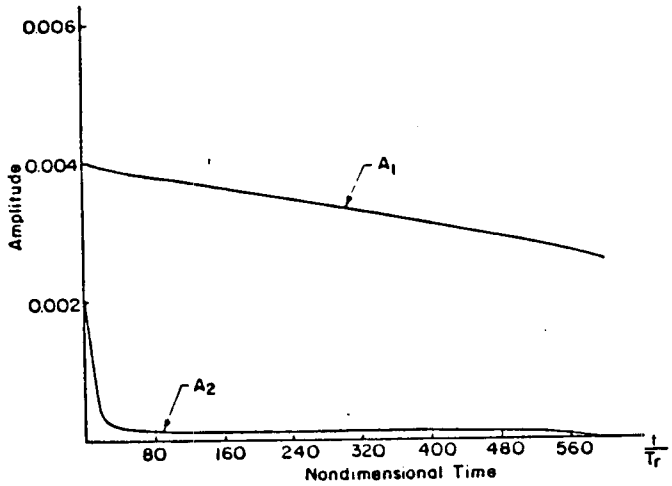

Fig. 13c THRESHOLD OF TRIGGERING

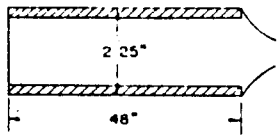

$r_e = a\left(\frac{P}{P_e}\right)^n$	$n = 0.5, a = 0.01\ ms^{-1}$	$\tau = 2\ 10^{-4} s$
$P_e = 1500$ psi	$\gamma = 1.23$	$a_1 = -10\ s^{-1}$
$T_e = 3000°k$	$K = 2.7\ 10^{-7} m^2 s^{-1}$	$a_2 = -500\ s^{-1}$
$N = 400$ Hz	$\rho s = 1.7\ 10^3 Kg m^{-3}$	$G_1 = -250\ s^{-1}$
$T_r = \frac{1}{N}$	$\omega = 2\pi N$	$G_2 = -2000\ s^{-1}$

Fig. 14a

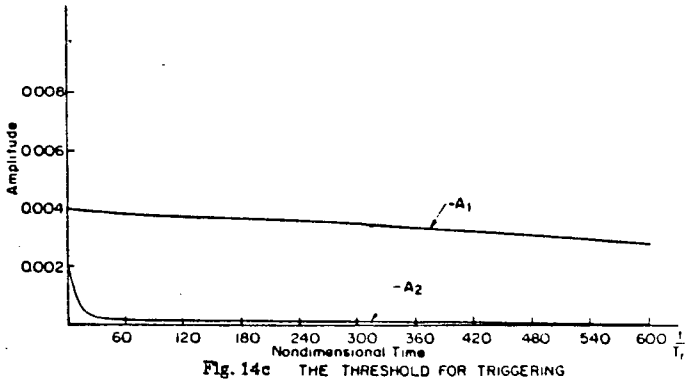

Fig. 14c THE THRESHOLD FOR TRIGGERING

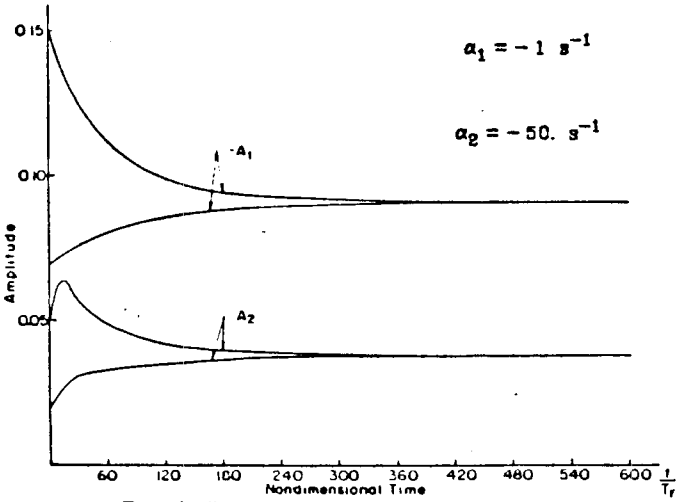

Fig. 14b TRIGGERING AND LIMIT CYCLE EXISTENCE

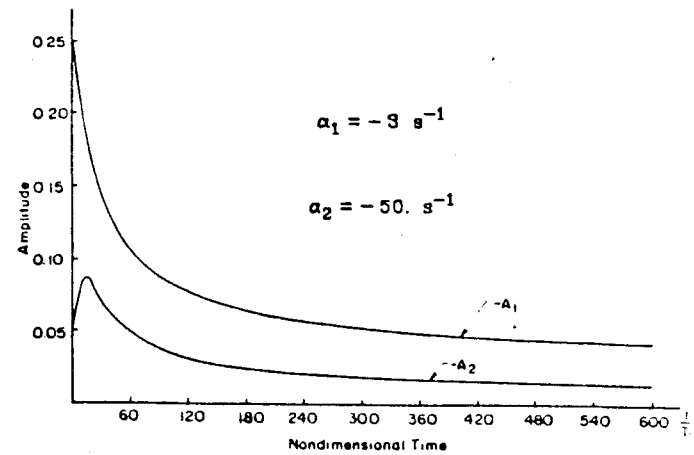

Fig. 14d SENSITIVITY OF TRIGGERING TO THE DECAY RATE OF THE FIRST MODE a_1